Journal of Nuclear Materials 438 (2013) S1266–S1270

Contents lists available at SciVerse ScienceDirect

Journal of Nuclear Materials

journal homepage: www.elsevier.com/locate/jnucmat

Can tokamaks PFC survive a single event of any plasma instabilities?

A. Hassanein *,[1], V. Sizyuk, G. Miloshevsky, T. Sizyuk

Center for Materials under Extreme Environment, School of Nuclear Engineering, Purdue University, 400 Central Drive, West Lafayette, IN 47907, USA

ARTICLE INFO

Article history:
Available online 16 January 2013

ABSTRACT

Plasma instability events such as disruptions, edge-localized modes (ELMs), runaway electrons (REs), and vertical displacement events (VDEs) are continued to be serious events and most limiting factors for successful tokamak reactor concept. The plasma-facing components (PFCs), e.g., wall, divertor, and limited surfaces of a tokamak as well as coolant structure materials are subjected to intense particle and heat loads and must maintain a clean and stable surface environment among them and the core/edge plasma. Typical ITER transient events parameters are used for assessing the damage from these four different instability events. HEIGHTS simulation showed that a single event of a disruption, giant ELM, VDE, or RE can cause significant surface erosion (melting and vaporization) damage to PFC, nearby components, and/or structural materials (VDE, RE) melting and possible burnout of coolant tubes that could result in shut down of reactor for extended repair time.

1. Introduction

Material erosion and damage due to intense energy deposition on target surfaces is important for many applications including thermonuclear fusion reactor design. Deposition of powerful plasma and particle beams (power densities up to hundreds of GW/m^2 and time duration of fraction of ms to tens of ms) due to loss of confinement on various materials significantly damages exposed surfaces and indirectly nearby components. Safe and reliable operation is still one of the major challenges in the development of new generation of ITER-like fusion reactors. The deposited plasma energy during major disruptions, giant edge-localized modes (ELMs), vertical displacement events (VDEs), and runaway electrons (REs) causes significant surface erosion, possible structural failure, and frequent plasma contamination. The overall damage depends on the detailed physics of plasma instabilities, the physics of plasma/material interactions, and the design configuration of plasma-facing components (PFCs) [1]. While plasma disruptions and ELM will have no significant thermal effects on the structural materials or coolant channels because of their short deposition time, VDE, having longer duration time, and runaway electrons (REs), having deeper penetration depth, could have destructive impact on these structural components as a result of the high heat flux reaching the coolant channels, possibly causing burnout of these tubes [2,3]. Additional bulk damage may include large temperature increases in structural materials and at the interfaces between surface coatings and structural materials. These large temperature increases can cause high thermal stresses, melting and detachment of surface coating material, and material fatigue and failure. In addition to these effects, the transport and redeposition of eroded surface materials to various locations on PFC are of major concern for plasma contamination, safety (dust inventory hazard), and successful and prolonged plasma operation after instability events [1].

Comprehensive efforts are continued developing the HEIGHTS simulation package to study self-consistently various effects of high particle and power transients on material operation and lifetime [2–5]. The enhanced HEIGHTS consists of several modules that integrate various stages of plasma material interaction starting from energy release from the bulk to scrape-off-layer and up to the transport of the eroded and splashed debris as a result of the deposited energy/particle fluxes. The integrated models predict material loss, PFC lifetime from transients, and contamination effects in real 3-D ITER geometry.

2. Damage due to giant ELMs and disruptions

To predict the response of disruptions and ELMs plasma impact on the divertor plate, comprehensive physical and numerical models are developed and implemented in HEIGHTS package. Bulk plasma energy released to SOL, energy deposition on divertor, divertor material erosion, stopping of plasma energy in eroded material and conversion into radiation in the shielding layer, then the resulting energy deposition of radiation flux to surrounding areas, evolution of vapor plasma temperature and density, resulting photon radiation and its transport, and deposition around the divertor and nearby components area are calculated selfconsistently for the predicted ELM and disruption parameters for realistic ITER geometry as shown in Fig. 1 [6]. The configuration/geometry

* Corresponding author.
E-mail address: hassanein@purdue.edu (A. Hassanein).
[1] Presenting author.

0022-3115/$ - see front matter © 2013 Elsevier B.V. All rights reserved.
http://dx.doi.org/10.1016/j.jnucmat.2013.01.281

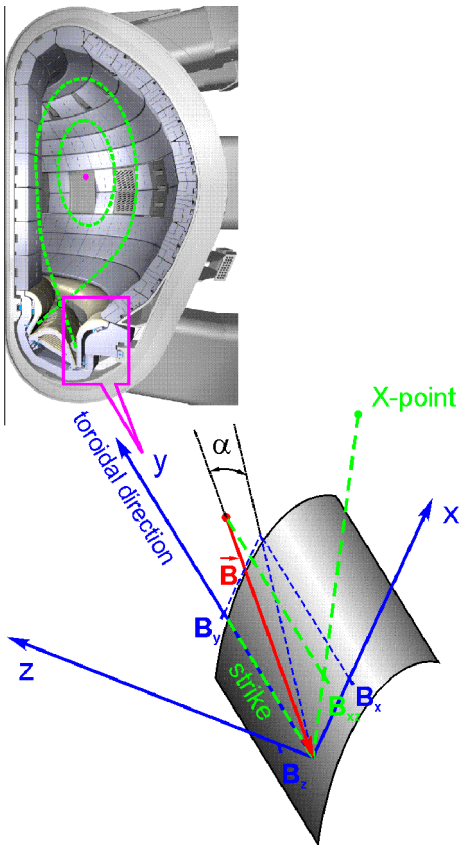

Fig. 1. Schematic illustration of coordinate system used to describe ITER geometry [4].

of tokamak wall and divertor components and the magnetic field structure are key factors in the performance of the tokamak fusion reactor.

The plasma impact is simulated in our Monte Carlo algorithm as deuterium–tritium plasma particles flow in magnetic field along the separatrix line. The spatial distribution of plasma impact is modeled exponentially along the strike point as described in Ref. [4]. The major radius in ITER geometry was 6.5 m and the initial temperature of the plasma was taken as 3.5 keV. Disruption and ELM durations of 0.1 ms and 1.0 ms were simulated [7,8]. The Monte Carlo algorithm included modeling of plasma particles interaction with divertor solid target, divertor vaporized material, and the developed divertor plasma in magnetic field. The magneto hydrodynamics (MHD) domain integrates modeling of plasma hydrodynamic evolution, magnetic diffusion, heat conduction, and radiation transport. Carbon plasma opacities were calculated using HEIGHTS atomic physics package and combined in 3800 spectral groups to provide maximum accuracy for photon transport calculations.

We compared the effect of a major disruption having 126 MJ total impact energy (100% pedestal energy) and a giant ELM (10% pedestal energy) on carbon divertor plate. The spatial distribution of the ELM and disruption plasma impact, modeled exponentially along the strike point, gives unshielded maximum energy deposition near the divertor strike point of 4.6 MJ/m^2 and 46 MJ/m^2 for ELM and disruption respectively. The final divertor surface erosion profiles are products of three time-dependent processes: direct initial energy impact from core/SOL plasma; secondary radiation of the evolving hot plasma cloud; and thermal heat conduction in divertor plate. The behavior of these processes depends on the total energy deposited and is different for short and long plasma impact durations. The shorter impact duration (0.1 ms) initiates intense surface vaporization. The produced plasma cloud has high temperature and is very effective in forming stable shield for incoming plasma particles because of insufficient time for vapor MHD motion and transport. This plasma shield acts as absorptive layer for incoming plasma particles. The incoming particles decelerate, scatter, strongly reradiate and deviate from the initial impinging direction in the plasma cloud that results in decrease in erosion depth directly at strike point but broadening of entire erosion area. Because plasma cloud is located near strike point and has relatively stable position, the second process of plasma radiation is evolved in this closed area around divertor strike point and relatively far from the nearby components. The initial impact energy at the shorter deposition time is consumed mostly in vaporization because of insufficient time for thermal conduction inside the divertor plate. Fig. 2 compares carbon surface vaporization profile for disruption and ELM at two deposition times, i.e., 0.1 ms and 1.0 ms. Increasing the deposited energy 10 times only increases maximum erosion depth by factor of 2–3. Shorter deposition time results in broader erosion profile along the divertor plate.

3. Damage due to vertical displacement events (VDEs)

Unlike disruptions and ELMs, VDEs cause significant surface and structural damage to PFC due to their longer durations. Like disruptions and ELMs, surface damage consists of vaporization, spallation, and liquid splatter of metallic materials. Structural damage includes large temperature increases and high thermal stresses in structural materials and the interface between coatings and structural components. The comprehensive 3-D model included in HEIGHTS is specifically developed to study the longer VDE plasma instabilities. The model includes detailed deposition processes, surface vaporization, phase change and melting, heat conduction to coolant channels, and critical heat flux criteria at the coolant channels [3].

The upgraded HEIGHTS package is used to simulate in full 3D laboratory experiments, current VDE in tokamak devices, and the response of entire ITER modules to VDE. A typical reactor-like VDE will have an incoming energy density of up to 60 MJ/m^2 deposited in 0.1–0.5 s (i.e., VDE power of 120–600 MW/m^2). The initial temperature distribution of the PFC and the bulk substrate prior to VDE is calculated according to the steady state heat flux, module design, and initial coolant temperature [3]. HEIGHTS were recently benchmarked against VDE in JET and simulation experiments using powerful electron beam and showed excellent agreement with the data [2,3].

Our simulation then used recent ITER design modules of copper alloy heat sink as structural material coated by beryllium and mounted on steel support structure with water coolant [9]. Plasma energy density with peak at 25 MJ/m^2 deposited over 0.8 s was considered in this analysis. The pressure in the 1.2 m long length coolant channel was constant about 3.0 MPa. The surface temperature of the copper-structure during VDE was calculated for different thicknesses of beryllium or tungsten coating materials at locations where VDE may strike. Fig. 3 shows Be surface temperature of 10-mm-thick Be coatings on top of 22-mm-thick Cu substrate and Cu interface temperature during VDE. Water flow velocity is assumed 10 m/s with inlet temperature of 115 °C. For reactor conditions, the coating/tile thickness is determined by surface temperature limitations during normal operation.

If we consider, however, the highest predicted energy load due to VDE, using tungsten coatings instead to reduce surface vaporization, the Cu surface interface will melt during VDE. For this condition, only Be coatings of reasonable thickness (about 5–10 mm) can withstand acceptable temperature rise in Cu structure, because most of incident plasma energy is removed due to higher surface

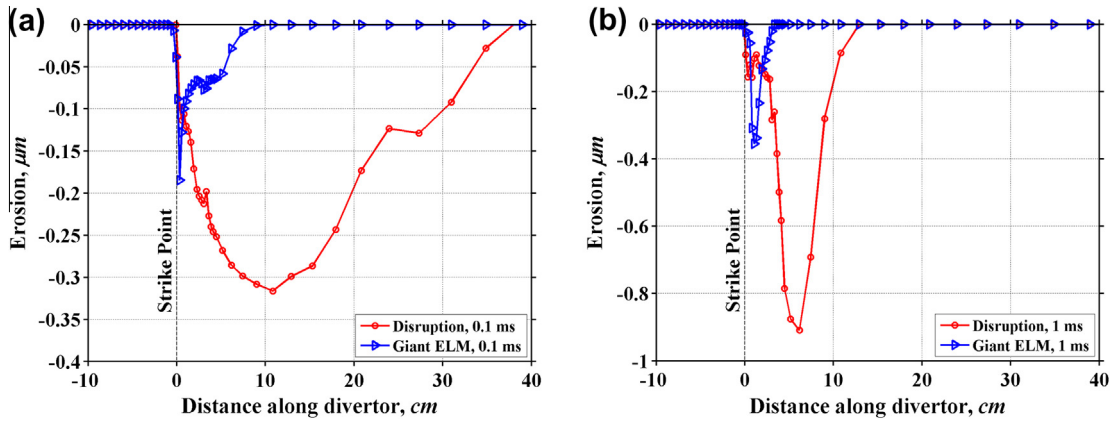

Fig. 2. Carbon erosion thickness along divertor plate for giant ELM and disruption at two different deposition times.

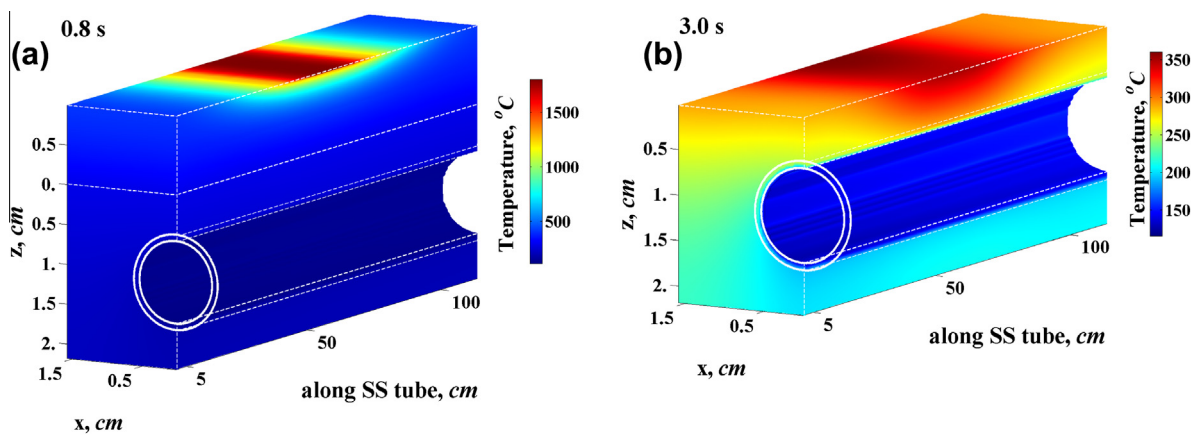

Fig. 3. Temperature distribution for surface heat loads with Gaussian profile in Be and Cu structures.

vaporization of Be, leaving less energy to be conducted through the structural material. Therefore, low-Z materials such as Be coatings will suffer significant surface erosion while protecting the structural copper substrate. Erosion thicknesses of up to 500 μm can be expected during VDEs expected range of parameters and possible melting of substrate and coolant burnout in locations where VDE can strike high-Z materials such as W [3,10].

4. Damage due to runaway electrons (REs)

The toroidal electric field in tokamaks gives rise to the runaway electrons phenomenon during the current phase of plasma disruptions. Due to the decrease of Coulomb collision frequency with increasing energy, electrons with energies larger than critical threshold are continuously accelerated by the electric field. The effect of runaway electrons impinging at vessel walls is strongly dependent on the energy gained in tokamak toroidal electric field. Detail energy deposition of RE module was implemented and benchmarked in HEIGHTS by taking into account various interaction mechanisms of energetic electrons with surface target atoms in strong and inclined magnetic field [5]. RE will have both parallel and perpendicular velocity components to the inclined magnetic field and arrive at the first wall surface in spiral motion. The geometry shown in Fig. 4 was used in our simulations. Thickness of armor material (Be or W) was assumed 10 mm. The Cu alloy thickness was taken as 22 mm. Stainless steel tubes had an internal diameter of 10 mm and an external one of 12 mm, pitch between neighboring tubes was 28 mm. Water coolant tubes were located

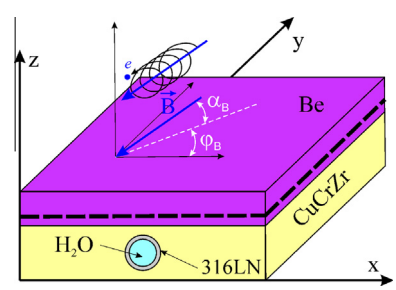

Fig. 4. Schematic illustration of wall design for RE analysis [5].

at the half-thickness of the heat sink. The magnetic field B in the three dimensional modeling space had two directional angles: incident angle α_B and azimuth angle φ_B. If RE strike W armor instead of Be, surface melting of W occurs for all parameters of runaway electrons considered in this study.

Fig. 5 compares the temperature response of Be coating and Cu/SS structure for two different RE energies of 10 and 50 MeV having energy density of 50 MJ/m^2 deposited in 10 ms duration. Lower RE energies deposit most of their energy in Be causing significant melting while higher RE energies penetrate Be coating and depositing larger part of their energies in Cu causing structure melting. Fig. 6 compares Be and W coating response to 50 MeV RE deposited in 10 ms. The high-Z tungsten coating absorbs most of the RE energies causing melting of W but protect and significantly reduce Cu structure temperature rise. As a mitigation method, using a thin tungsten insert layer in between Be armor and Cu structure pre-

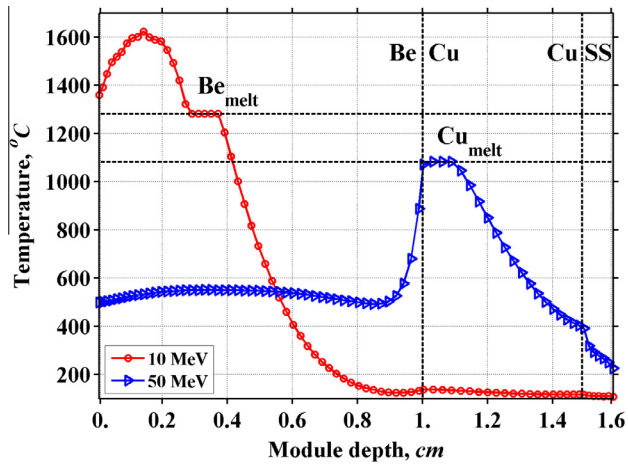

Fig. 5. Temperature rise in Be and Cu structure.

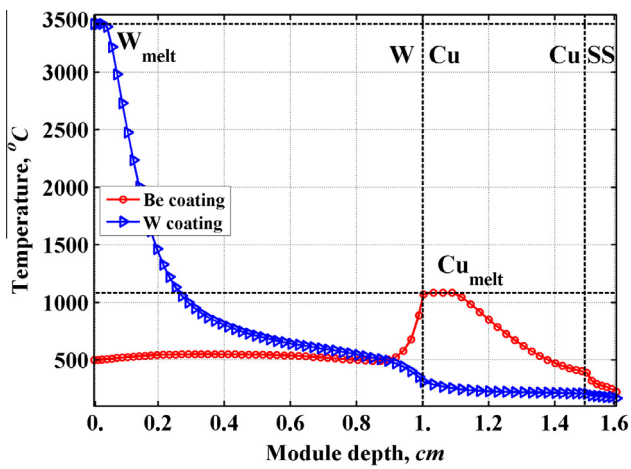

Fig. 6. Temperature rise in W and Cu structure.

vents melting of all structure for the parameters considered. RE detail parameters and strike location and design are very important in assessing the damage.

5. Melt layer erosion during plasma instabilities

Melt layer losses during plasma instabilities on metallic PFCs can further reduce lifetime and contaminate the plasma. Mechanisms causing melt layer erosion and splashing include hydrodynamic instabilities at the melt layer surface and bubble formation and splashing due to superheating. An important loss mechanism is development of Kelvin–Helmholtz (K–H) instability. Perturbations of plasma-melt interface and development of waves can be produced by the high-speed plasma flowing along the thin melt layer. The K–H instability arising at the plasma-melt interface can result in droplets splashed into the plasma. The inviscid and viscous stability mode analysis are both used to predict development and growth of surface waves at the plasma-liquid metal interface. The capillary droplet model is then applied to estimate melt losses.

The inviscid linear stability analysis [11,12] predicts that the development of the K–H instability, growth of waves, and droplet ejection from melt layer due to VDEs are unlikely under tokamak conditions ($N_p \leqslant 10^{20}\,\mathrm{m}^{-3}$). Streams of plasma with velocities >40 km/s are required to trigger K–H instability. These velocities are significantly higher than plasma velocities of VDEs (less than 130 m/s in the vertical direction and 80 m/s in the radial direction) estimated in the JT-60U tokamak [13]. The wavelength of the fastest "dangerous" growing wave is on the order of >1 cm, that is large compared to the thickness of melt layer 0.5–2 mm.

The inclusion of small but finite plasma viscosity has significant influence on stability of melt layer according to viscous potential flow theory [14]. Our analysis predicted that viscosity has significant destabilizing effect. For viscous plasma-melt flow under tokamak conditions, the critical velocity is greatly reduced. With increase of viscosity, the critical velocity is also slightly shifted toward shorter waves of 1–2 cm. The viscous plasma streaming with velocity around 100 m/s can accelerate growth of waves on Be melt layer, for example, with wavelength around μm size on timescales of μs, thus causing melt splashing and droplet ejection. Therefore, the capillary droplet model [11,15] based on assumptions that the fastest growing wavelength is much smaller than the thickness of melt and droplets generated at the peaks of these short waves dragged away by plasma wind is not applicable under ITER conditions. According to this inviscid theory a capillary instability (μm-size wavelength) is completely suppressed.

The outcomes of the viscous potential flow analysis of K–H instability are used in the capillary droplet model [11] to estimate erosion rate and losses of Be melt. Viscous plasma flowing over melt surface with velocities 80–100 m/s can generate the fastest growing waves with wavelengths 20–100 μm that is much smaller compared to the thickness of Be melt of 0.5–2 mm. Thus, droplets can be formed due to breakaway of melt at peaks of these short surface waves. This makes the capillary droplet model applicable for estimations of melt losses. The thickness of removed melt as a function of the relative velocity is shown in Fig. 7 for different values of plasma viscosity. The horizontal black line indicates a maximum thickness of Be melt of $h_m = 2$ mm observed in experiments. For plasma with large viscosity, $\sim 10^{-5}$ kg/(m s), melt layers with large thickness >4 mm can be removed during VDEs with duration $\tau = 0.1$ s. At lower plasma viscosity, $\sim 10^{-6}$ kg/(m s), thickness of Be melt around 1–2 mm can be lost due to VDEs plasma with displacement velocity 100–120 m/s. At larger displacement velocity, the whole depth of melt layer can be affected during $\tau = 0.1$ s. For plasma with even lower viscosity $\sim 5 \times 10^{-7}$ kg/

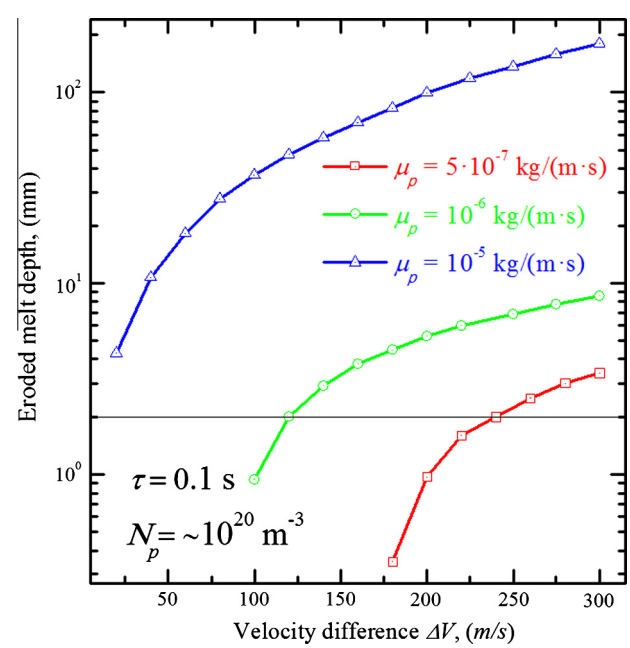

Fig. 7. Thickness of Be melt eroded by plasma as a function of relative velocity and plasma viscosities.

(m s) and flowing with velocity 160–240 m/s, the lost melt can be 0.3–2 mm. Viscous plasma with velocity >240 m/s is required to remove thicker Be melt.

In summary, we find the capillary droplet model based on viscous potential flow theory predicts that viscous plasma with displacement velocities 100–120 m/s is capable of removing Be melt layer with thickness about 2 mm during VDEs with effective duration $\tau = 0.1$ s. The predictions of this phenomenological model should be considered as qualitative estimates due to extension of the linear stability analysis to non-linear mode when droplets are formed, and to the uncertainty in plasma parameters such as velocity, density, and viscosity [16]. The viscous potential flow analysis indicates the crucial effect of plasma viscosity on the melt stability. Experimental work is needed to clarify the role of plasma viscosity in K–H instability and loss of melt layers.

6. Conclusions

We used our upgraded HEIGHTS simulation package to study the impact of various plasma instabilities such as disruption, ELM, VDE, and RE on plasma facing components in realistic ITER-like reactor conditions and configurations. Simulation results showed strong influence of the 3D MHD effects on disruption and ELM divertor erosion dynamics in the dome area. Radiation fluxes to nearby locations from the shielding cloud have similar magnitude as energy depositions at the divertor surface. This highlights the additional damage risk of nearby surfaces during giant ELMs and disruption in ITER-like closed configuration. VDE and RE can cause large surface erosion as well as significant temperature rise at the structural interface and coolant channels which can cause extended reactor downtime. While surface erosion may be easier to repair compared to structural damage, surface erosion products from both vaporization and splashed droplets of metallic surface components can significantly contribute to plasma contamination and may prohibit successful operation following these instability events. Overall, various plasma instabilities must be eliminated or significantly reduced/mitigated for the magnetic fusion energy concept to be attractive.

Acknowledgment

Work is supported by the US Department of Energy, Office of Fusion Energy Sciences.

References

[1] A. Hassanein, Fusion Eng. Design 60 (2002) 527.
[2] A. Hassanein, T. Sizyuk, M. Ulrickson, Fusion Eng. Design 83 (2008) 1020.
[3] A. Hassanein, T. Sizyuk, Nucl. Fusion 48 (2008) 115008.
[4] V. Sizyuk, A. Hassanein, Nucl. Fusion 50 (2010) 115004.
[5] V. Sizyuk, A. Hassanein, Nucl. Fusion 49 (2009) 095003.
[6] R.A. Pitts et al., J. Nucl. Mater. 415 (2011) S957–S964.
[7] T.C. Hender et al., Nucl. Fusion 47 (2007) S128–S202.
[8] G. Federici et al., Plasma Phys. Control Fusion 45 (2003) 1523–1547.
[9] P. Lorenzetto, F. Zacchia, Blanket Information Meeting, Barcelona, 2010.
[10] A. Hassanein, Fusion Technol. 30 (1996) 713.
[11] G. Miloshevsky, A. Hassanein, J. Nucl. Mater. 415 (2011) 74–77.
[12] G. Miloshevsky, A. Hassanein, Nucl. Fusion 50 (2010) 115005.
[13] M. Matsukawa et al., Fusion Eng. Design 23 (1993) 341–349.
[14] T. Funada, D.D. Joseph, J. Fluid Mech. 445 (2001) 263–283.
[15] Y. Shi, G. Miloshevsky, A. Hassanein, J. Nucl. Mater. 412 (2011) 123–128.
[16] G. Miloshevsky, A. Hassanein, these proceedings.